Extended Abstracts of the 2001 International Conference on Solid State Devices and Materials, Tokyo, 2001, pp. 384–385

F-5-2

Enhanced Quantum Effect for Sub-0.1 μm Pocket Technologies and Its Relevance for the On-Current Condition

K. Morikawa, H. Ueno[1], D. Kitamaru[1], M. Tanaka[1], T. Okagaki[1], M. Miura-Mattausch[1], H. J. Mattausch, S. Kumashiro[2], T. Yamaguchi[2], K. Yamashita[2] and N. Nakayama[2]

Research Center for Nanodevices and Systems and [1]Faculty of Engineering, Hiroshima University
1-4-2, Kagamiyama, Higashi-Hiroshima, 739-8527, Japan
Phone: +81-824-24-6265 Fax: +81-824-22-7185 E-mail: morikawa@sxsys.hiroshima-u.ac.jp
[2]Semiconductor Technology Academic Research Center, 3-17-2, Shin-Yokohama, Kanagawa, 222-0033, Japan

1. Introduction

The pocket-implant technology is promising for coming MOSFET generations [1–4], because the abrupter lateral channel/contact junctions can suppress short-channel effects (SCE) down to 25nm gate length (L_g) [2]. On the other hand, the quantum effect (QE) is also becoming remarkable with down scaling. It has been demonstrated that the inverse capacitance induced by QE causes a serious gate-voltage drop, which is usually modeled as an increase of the effective oxide thickness Δt_{ox} [5]. However, previous QE investigations have only treated the off-current condition. Here we analyze QE under the normal on-current operating condition for pocket-implanted MOSFETs.

2. Optimization of the Pocket Profile

A new analytical threshold voltage (V_{th}) model of pocket implanted MOSFETs is based on the idea of V_{th} determination by the sum of carrier concentrations induced both in pocket and non-pocket regions [6]. Two parameters for the pocket profile ($N_{sub,p}$: maximum concentration; L_p: length of pocket penetration into the channel) are extracted from measured V_{th}-L_g characteristics. At increased drain voltage (V_{ds}) the channel conduction due to the lateral electric field, also included in the model, becomes important and the contribution of the drain-side pocket decreases. Fig. 1 compares V_{th} calculated by the model and measurements for a 0.1 μm technology with 2.8nm oxide thickness.

We use this new V_{th}-model to extrapolate to an optimized pocket profile for a 70nm technology on the basis of the results shown in Fig. 1. According to the SIA roadmap, t_{ox} and target V_{th} (long channel) are fixed to 1.5 nm and 0.2V, respectively. The extrapolation follows 3 steps: (i) The V_{th}-L_g characteristics are calculated with the developed V_{th} model, and optimal L_p and $N_{sub,p}$ are chosen. (ii) The 2D pocket profile is then optimized with the chosen L_p and $N_{sub,p}$ [7]. (iii) With the 2D profile QE is estimated. Steps (i)–(iii) are iterated until a self-consistent solution is obtained.

The result is depicted in Fig. 2. Fig. 2 b shows the optimized pocket profile for the 70 nm-channel MOSFET. The optimal pocket penetration into the channel is up to the channel middle of L_g=70nm to enhance the reverse SCE (RSCE). The V_{th}-change is given by $\Delta V_{th}(L_g)$ $=\Delta V_{th,SCE}(L_g) + \Delta V_{th,RSCE}(L_g) + \Delta V_{th,QE}(L_g)$. We focus here on $\Delta V_{th,QE}$, which has not been considered previously. The fact that $\Delta V_{th,QE}(L_g)$ amounts to about 20% of $\Delta V_{th,RSCE}$ as shown in Fig. 3, allows to realize the required V_{th}-L_g characteristics with reduced $N_{sub,p}$. Our optimized profile shows a factor 2 lower pocket concentration than necessary without the QE contribution.

However, these results are obtained under off-current condition. An important question is whether this effect is preserved also under on-current condition.

3. Quantum Effect at On-Current Condition

To include QE in the on-current condition we have to solve the Schrödinger, the Poisson, the current-density and the continuity equation at least in 2D. However, this is very computer-time consuming and it is also difficult to achieve stable solutions. Therefore, we solve the Schrödinger equation after obtaining a solution for the other three equations. This is done iteratively. Fig. 4 a shows the results along the channel at V_{ds}=50mV and $V_{gs}=V_{th}+0.5$V. For comparison, results with an analytical equation [8] are depicted in the same figure

$$t_{ox}^{eff} = t_{ox} + \alpha \left(Q_b + \frac{11}{32} Q_i \right)^{-\frac{1}{3}} \quad (1)$$

where Q_b and Q_i are the depletion and the inversion charge, respectively. α is determined by the effective mass. The analytical solution of eq. (1) is derived with a triangular potential approximation perpendicular to the channel and occupation of only the lowest energy level. Analytical and self-consistent calculation results are similar. This means the approximations are good enough. However, with increasing V_{ds}, the triangular shape of the potential distribution disappears especially as the position moves from source to drain as demonstrated in Fig. 4 b. Fig. 5 compares energy-level results with the self-consistent simulation for V_{ds}=50mV and V_{ds}=1.2V. Without QE the ground state coincides with the potential bottom. Therefore we define the strength of QE by the energy difference between the potential bottom and the ground state. This difference is plotted in Fig. 6 a along the channel. The difference has a peak at the channel middle for V_{ds}=50mV due to the pocket implantation. The large reduction of the difference at the drain edge for V_{ds}=1.2V means that the quantization is getting lost. In fact, the confinement of carriers is weakened at the drain edge as shown in Fig. 6 b. This means that the on-current quantization is smaller than expected from the usual off-current calculation.

To examine the influence of the change of the QE strength along the channel on the I-V characteristics, we perform a Monte Carlo simulation with FALCON considering QE by modifying the potential bending to reproduce the carrier distribution (Fig. 6 b) and the surface-roughness-scattering rate. These modifications are calibrated so that the bulk mobility preserves the mobility universality. Fig. 7 shows the results for L_g=70nm. The reduction of I_{ds} including QE is partly due to the mobility reduction, which is not well verified yet. Nevertheless, it is obvious that the inclusion of the position dependent QE and the approximation of a homogeneous QE along the channel determined at the source side lead to equivalent results. The enhancement of $\Delta V_{th,QE}$ for V_{ds}=1.2V is mainly due to a shift of the position determing V_{th} to the source side to a higher pocket concentration.

4. Conclusion

We have demonstrated that the pocket implantation causes an enhanced QE with reduced L_g under the off-

current condition. Under the on-current condition QE becomes very position dependent. However, this dependence has a small influence on the on-current.

References

[1] Y. Taur and E.J. Nowak, IEDM Tech. Dig., p.215, (1997).
[2] Y. Taur *et al.*, IEDM Tech. Dig., p.789, (1998).
[3] H. -H. Vuong *et al.*, IEEE EDL, **21**, 5, p.248, (2000).
[4] H. Wakabayashi *et al.*, IEDM Tech. Dig., p.49, (2000).
[5] S. Takagi *et al.*, IEDM Tech. Dig., p.619, (1998).
[6] D. Kitamaru *et al.*, SISPAD 2001.
[7] M. Suetake *et al.*, Proc. SISPAD '99, p.207, (1999).
[8] Z. Yu *et al.*, Proc. IWCE-6 '98, p.222, (1998).

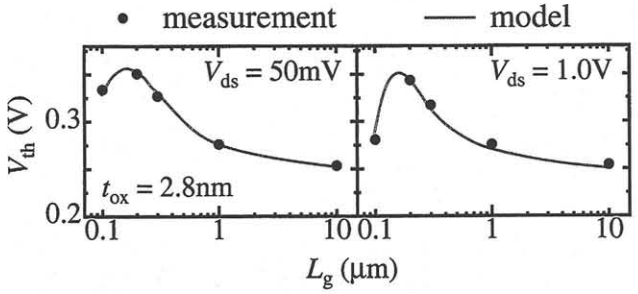

Fig. 1: Measured and simulated V_{th} dependence on L_g by using the developed V_{th} model for pocket implanted MOSFETs.

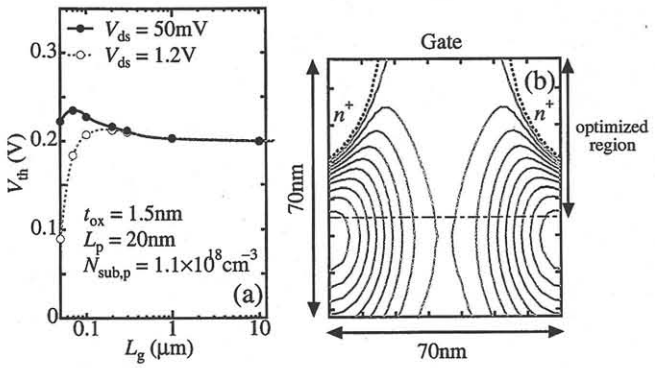

Fig. 2: (a) Optimized V_{th} dependence on L_g for a 70 nm technology with t_{ox}=1.5nm. (b) Pocket profile contours are optimized by approximating a Gaussian function. Contour lines are plotted from 6×10^{17} cm^{-3} to 4.2×10^{18} cm^{-3}.

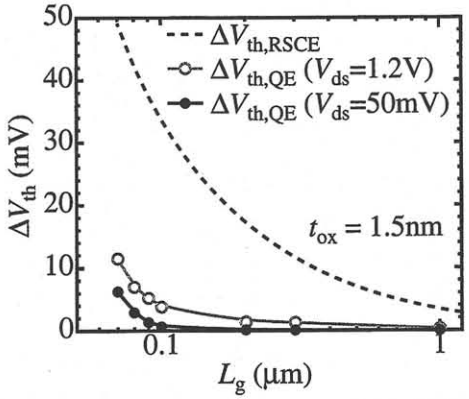

Fig. 3: Simulated increments $\Delta V_{th}(L_g)$=$V_{th}(L_g)$-$V_{th}(L_g$=10μm) for t_{ox}=1.5nm.

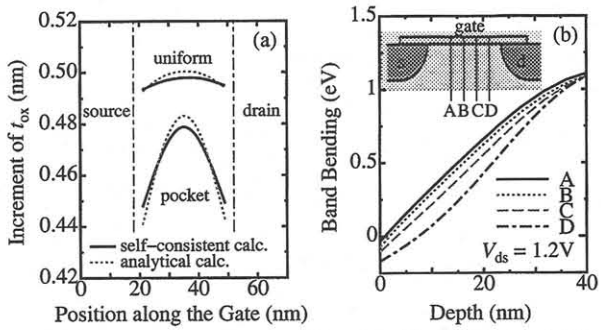

Fig. 4: (a) Increment of t_{ox} at V_{ds}=50mV. (b) Potential band bending at V_{ds}=1.2V.

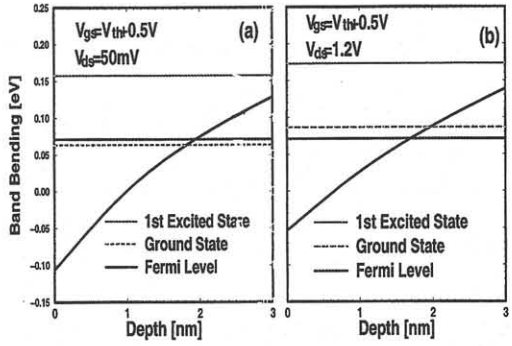

Fig. 5: (a) Potential band bending and eigen-values at V_{ds}=50mV, and (b) at V_{ds}=1.2V. These results are obtained at mid-channel position.

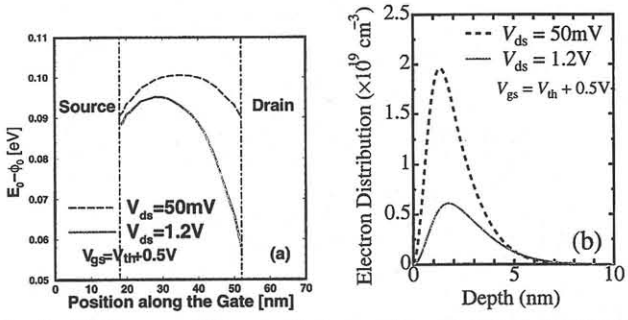

Fig. 6: (a) Energy difference between the ground-state energy of the longitudinal mode and the potential at the channel surface. (b) Electron distribution from surface to bulk at the drain edge.

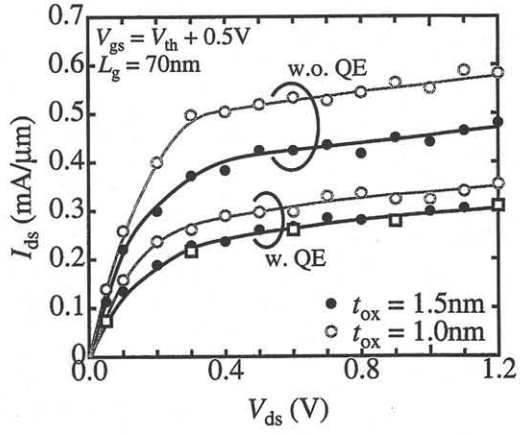

Fig. 7: I_{ds}-V_{ds} Characteristics by Monte Carlo Simulation for L_g=70nm. The results with squares consider the position dependent QE, whereas those with circles are for homogeneous QE along the channel.